Water Dynamics at the Interface in AOT Reverse Micelles

David E. Moilanen, Emily E. Fenn, Daryl Wong, and M. D. Fayer*

Department of Chemistry, Stanford University, Stanford, California 94305

Received: March 4, 2009; Revised Manuscript Received: April 23, 2009

The orientational dynamics of water molecules at the interface in large Aerosol-OT (AOT) reverse micelles are investigated using ultrafast infrared spectroscopy of the OD stretch of dilute HOD in H_2O. In large reverse micelles (~9 nm diameter or larger), a significant amount of the nanoscopic water is sufficiently distant from the interface that it displays bulk-like characteristics. However, some water molecules interact with the interface and have vibrational absorption spectra and dynamics distinct from bulk water. The different characteristics of these interfacial waters allow their contribution to the data to be separated from the bulk. The infrared absorption spectrum of the OD stretch is analyzed to show that the interfacial water molecules have a spectrum that peaks near 2565 cm^{-1} in contrast to 2509 cm^{-1} in bulk water. A two-component model is developed that simultaneously describes the population relaxation and orientational dynamics of the OD stretch in the spectral region of the interfacial water. The model provides a consistent description of both observables and demonstrates that water interacting with the interface has slower vibrational relaxation and orientational dynamics. The orientational relaxation of interfacial water molecules occurs in 18 ± 3 ps, in contrast to the bulk water value of 2.6 ps.

I. Introduction

Many of the important physical and chemical processes in a wide range of fields including biology, geology, and chemistry occur at and near aqueous interfaces. Transport of material through a cell membrane, erosion and dissolution of minerals, and heterogeneous catalysis are all governed by the dynamic interactions of small molecules with a surface. Often, this small molecule is water due to its importance as a part of all biological and many other natural systems. Water's flexible hydrogen-bonding network, which can rearrange to accommodate interfaces on an ultrafast time scale, makes dynamics at aqueous interfaces quite difficult to study. There are two key questions to address when studying aqueous interfaces. First, how are the dynamics and structure of water modified at the interface, and second, how far does the perturbation extend away from the interface. These questions are particularly important in crowded biological systems in which only a few molecular layers of water molecules separate large biomolecules and biomolecular structures.

Molecular dynamics (MD) simulations have studied hydration water extensively, concluding that most of the perturbation induced by an interface extends only a few molecular layers.[1−4] In an experiment, it is often difficult to separate the contribution of the interfacial water from the overwhelming background of bulk water. Several techniques, including Auger electron yield X-ray absorption spectroscopy,[5] sum frequency generation,[6] and various microscopy techniques, can provide structural information about interfaces. However, it is much more difficult to selectively probe the dynamics of water at an interface. Magnetic relaxation dispersion techniques have been utilized to selectively probe the dynamics of water at the surface of proteins and macromolecules.[4,7] While this technique is quite sensitive and able to detect the signature of very few water molecules, it does not have the time resolution to probe the dynamics of water on the time scale that they occur. Ultrafast infrared spectroscopy has proven to be an extremely useful tool for probing the dynamics of water both for its femtosecond time resolution and for its ability to selectively probe water molecules with different absorption frequencies corresponding to different local environments.[8−22]

Recently, ultrafast infrared spectroscopy has been used to study water in a variety of nanoconfined systems, in which the dynamics of water are dominated by the effects of the interface.[10,12,13,15,21] Many of these studies have focused on the dynamics of water confined in reverse micelles formed by the surfactant Aerosol-OT (sodium bis(2-ethylhexyl) sulfosuccinate). AOT forms well-characterized nominally monodispersed spherical reverse micelles in isooctane over a large range of water content from essentially dry up to ~60 water molecules per AOT.[23] The number of water molecules per AOT is conveniently described using the w_0 parameter, $w_0 = ([H_2O])/([AOT])$. The smallest reverse micelles have radii of less than 1 nm (50−100 waters), while the largest have radii of up to 14 nm (~400 000 waters). With this large size range, it is possible to change the relative amount of the water interacting directly with the interface from a large fraction to a small fraction of the total by increasing the reverse micelle size.

Over the past few years various authors have shown that the properties of water confined in AOT reverse micelles can be described using a core/shell model in which a shell of water molecules interacting directly with the interface have an absorption spectrum, vibrational lifetime, and orientational dynamics that are distinct from the more bulk-like water found in the center of the reverse micelle water pool.[15,21,22,24,25] Piletic et al. presented a detailed study of the absorption spectrum and vibrational lifetime of dilute HOD in H_2O and showed that these two observables were well described for all reverse micelles using a superposition of the data for the smallest reverse micelle and bulk water.[15] It was also shown that the orientational dynamics in the very small reverse micelles were quite different from those of bulk water.[15] Bakker and co-workers, studying the OH stretch of HOD in D_2O, later showed that the orientational dynamics in larger reverse micelles could be

* To whom correspondence should be addressed. E-mail: fayer@stanford.edu.

10.1021/jp902004r CCC: $40.75
Published on Web 06/01/2009

described with a two-component model in which the orientational dynamics in the shell were different than the core but not the same as the smallest reverse micelle.[21] They showed that it was possible to obtain information on the orientational dynamics in the shell (interfacial water) and gave a lower bound of ~15 ps for the water orientational relaxation time.[21] The broad OH stretch band utilized in these experiments has the advantage of greater spectral separation between the core and the shell due to its larger line width. However, the fast vibrational relaxation of the OH stretch only allowed data to be collected over a limited time interval.

Here we present a comprehensive wavelength-dependent study of the OD stretch of HOD in H_2O confined in large AOT reverse micelles with the goal of accurately determining the reorientation time of water molecules interacting with the interface of the reverse micelle. The OD stretch has a lifetime that is approximately twice as long as the OH stretch, which allows data to be collected over a much longer interval. Since the orientational dynamics of HOD are largely independent of whether the remainder of the water is D_2O or H_2O,[9] the longer vibrational lifetime of OD permits an accurate determination of the long time orientational dynamics of the interfacial water. Large reverse micelles ($w_0 = 46$, 37, and 25 with radii = 10, 8.5, and 4.5 nm) were chosen for this study to ensure that a significant bulk-like pool exists in the center of the reverse micelle. Laage and Hynes have shown that the orientational dynamics of a water molecule depend on the motions of water molecules in its first and second solvation shell.[26,27] On the basis of this model, the water in the core of a large reverse micelle should have bulk characteristics because the water is spatially well separated from the interface and has first and second solvation shells that also do not interact with the interface. This criterion does not apply for smaller reverse micelles, which will be discussed in a subsequent publication.

The manuscript is organized as follows. We first analyze the infrared spectrum of the OD stretch to identify the spectral region in which interfacial water molecules will have a non-negligible contribution to the signal. Next, the important characteristics of the core and shell are discussed and a two-component model is developed to describe the population relaxation and orientational dynamics. Finally, the two-component model is applied to extract the population relaxation and orientational dynamics of the interfacial water.

II. Experimental Section

AOT, isooctane, H_2O, and D_2O (Aldrich, Inc.) were used as received. A 0.5 M stock solution of AOT in isooctane was prepared, and the residual water content in the stock solution was determined by Karl Fischer titration to be 0.5 water molecules per AOT ($w_0 = 0.5$). A stock solution of 5% HOD in H_2O was added to measured amounts of the 0.5 M stock solution to prepare reverse micelles with the desired w_0. Three sizes of reverse micelles were studied, $w_0 = 25$, 37, and 46. The radii of these reverse micelles have been determined by photon correlation spectroscopy and are ~ 4.5, 8.5, and 10 nm, respectively.[23] Samples for infrared absorption and ultrafast IR experiments were housed in sample cells between two CaF_2 windows separated by a Teflon spacer. The thickness of the spacer was selected to maintain an optical density of ~0.5 in the OD stretch region for all samples. Studying the OD stretch of dilute HOD in H_2O is important to eliminate vibrational excitation transfer that causes artificial decay of the orientational correlation function in either pure H_2O or D_2O.[28,29]

The laser system used for these experiments consists of a Ti:Sapphire oscillator and regenerative amplifier pumping an OPA and difference frequency stage to produce ~70 fs pulses at ~4 μm (2500 cm^{-1}). The mid-IR light was split into an intense pump pulse and a weak probe pulse. Before the sample, the polarization of the pump pulse is rotated from horizontal to 45° relative to the horizontally polarized probe. The pump pulse is passed through a polarizer set to 45° immediately before the sample to ensure that the HOD molecules are excited by a linearly polarized pump pulse. The polarization of the probe is resolved parallel and perpendicular (+45° and −45° relative to horizontal) to the pump after the sample using a computer-controlled rotation stage. Another polarizer immediately after the resolving polarizer and just before the input to the monochromator is used to set the polarization entering the monochromator to horizontal to eliminate differences in the polarization-dependent reflection and diffraction efficiencies in the monochromator.[30] The probe is frequency dispersed by the monochromator and detected using a 32-element MCT detector (Infrared Associates and Infrared Systems Design). The pump−probe signal measured parallel ($I_{||}$) and perpendicular ($I_\perp$) to the pump contains information about both the population relaxation and the orientational dynamics of the HOD molecules.[31]

$$I_{||} = P(t)(1 + 0.8C_2(t)) \quad (1)$$

$$I_\perp = P(t)(1 - 0.4C_2(t)) \quad (2)$$

$P(t)$ is the vibrational population relaxation, and $C_2(t)$ is the second Legendre polynomial orientational correlation function. Pure population relaxation can be extracted from the parallel and perpendicular signals using

$$3P(t) = I_{||} + 2I_\perp \quad (3)$$

In the case of a single ensemble of molecules undergoing orientational relaxation, the orientational correlation function, $C_2(t)$, can be determined from the anisotropy, $r(t)$, by

$$r(t) = (I_{||} - I_\perp)/(I_{||} + 2I_\perp) = 0.4C_2(t) \quad (4)$$

The additional complications that arise in calculating the anisotropy when two distinct subensembles of molecules exist in the system will be discussed in detail below.

III. Results and Discussion

A. Identifying the Spectral Region and Characteristics of Interfacial Water. The infrared absorption spectrum of water in AOT reverse micelles has been analyzed by a number of authors.[15,32−35] Many of these studies focused on the OH stretching region of H_2O, which is complicated by a Fermi resonance as well as overlapping symmetric and antisymmetric stretching modes.[32−34] The uncoupled OD or OH stretching mode of HOD in H_2O or D_2O with its single, featureless band provides a much less complicated spectrum.

Here, our purpose is to identify the spectral region that is most likely to contain the maximum amount of information about water molecules interacting with the interface of the reverse micelle. The IR spectra of several large reverse micelles ($w_0 = 46$, 37, 25), bulk water, and the $w_0 = 2$ reverse micelle are shown in Figure 1a. Even in the large reverse micelles there is a contribution from ODs interacting with the interface, which manifests itself by a slight blue shift of the absorption spectrum. As the reverse micelle size decreases, the blue shift becomes

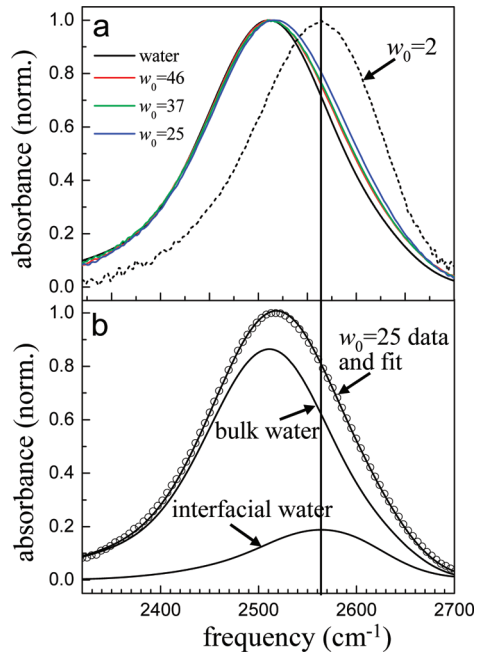

Figure 1. (a) Infrared absorption spectrum of the OD stretch of dilute HOD in H_2O in several large AOT reverse micelles, bulk water, and the $w_0 = 2$ reverse micelle: Water (solid black line), $w_0 = 46$ (red), $w_0 = 37$ (green), $w_0 = 25$ (blue), and $w_0 = 2$ (dashed black line). (b) Infrared absorption spectrum of the $w_0 = 25$ reverse micelle and a two-component fit consisting of the spectrum of bulk water and the $w_0 = 2$ reverse micelle. The only adjustable parameter is the relative amplitude of the two spectra. The solid vertical line marks the peak of the $w_0 = 2$ spectrum in both figures (2565 cm^{-1}). The region with the largest contributions from interfacial water molecules will be at frequencies higher than this line.

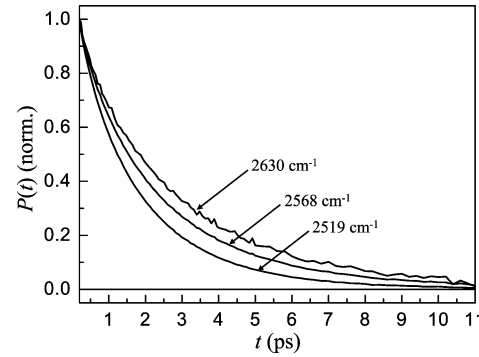

Figure 2. Vibrational population relaxation decays at several frequencies for the $w_0 = 25$ reverse micelle.

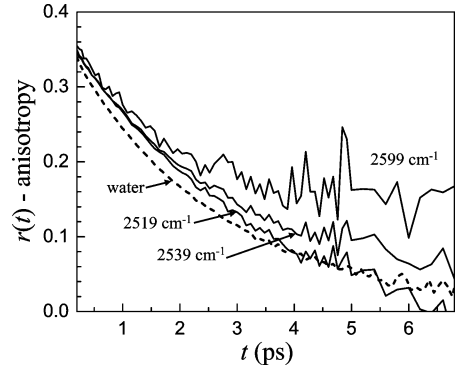

Figure 3. Anisotropy decays at several frequencies for the $w_0 = 46$ reverse micelle with the anisotropy decay of bulk water (dashed line) for comparison. The anisotropy decays slow as the frequency increases.

more apparent, and for the $w_0 = 2$ reverse micelle the absorption spectrum peaks at ~2565 cm^{-1}. The blue shifting of the absorption spectrum with decreasing w_0 demonstrates that the OD stretching frequency shifts to the blue when water molecules interact with the reverse micelle interface.

In the core/shell model applied by Piletic et al., the core spectrum was modeled as the bulk water spectrum and the shell spectrum was modeled as the spectrum of the $w_0 = 2$ reverse micelle.[15] In the large reverse micelles, the core spectrum should certainly be well represented by the spectrum of bulk water due to the extended hydrogen-bonding network in the center of the reverse micelle; it is not clear that the spectrum of interfacial waters should be that of the $w_0 = 2$ reverse micelle. MD simulations show that at small w_0 the interface is a rigid lattice with the sodium counterions strongly bound between sulfonate headgroups.[36] IR spectroscopy of the sulfonate stretching region[35] shows that the interaction between water molecules and the interface changes dramatically up to $w_0 \approx 5$, and many other authors have reported that 4−6 water molecules are required to solvate the sulfonate headgroup.[32,37,38] Therefore, it is likely that the spectrum of interfacial water in large reverse micelles is not exactly the same as the $w_0 = 2$ reverse micelle. However, the $w_0 = 2$ spectrum can be a useful guide to help identify the likely spectral region of interfacial water.

Figure 1b shows the results of a fit to the spectrum of the $w_0 = 25$ reverse micelle using a linear combination of the bulk water spectrum and the $w_0 = 2$ spectrum. The fit is quite good, showing that in spite of changes that occur at the interface as reverse micelle size increases, interfacial water is most likely to contribute to the pump−probe signal at frequencies higher than 2565 cm^{-1}.

Figure 2 shows the vibrational population relaxation of water in the $w_0 = 25$ reverse micelle at frequencies ranging from 2519 cm^{-1} at the center of the line to 2630 cm^{-1} on the blue side. These data are representative of the trends observed in the $w_0 = 37$ and 46 reverse micelles as well. The data in Figure 2 have been corrected for a small, well-documented isotropic heating contribution.[39,40] It is clear from the data that the vibrational relaxation is slower on the blue side of the line, the same spectral region associated with interfacial water in the IR spectrum. This indicates that water molecules at the interface have slower vibrational relaxation than bulk water.

Figure 3 shows the wavelength dependence of the orientational dynamics of water in the $w_0 = 46$ reverse micelle with bulk water for comparison. In the center of the absorption line, the anisotropy decay is fast but becomes progressively slower as the OD stretch absorption frequency increases, appearing to reach a plateau after ~4 ps for the 2599 cm^{-1} data, which has a significant contribution from the interfacial spectral region. This apparent plateau does not mean that the orientational dynamics of water in the interfacial region are too slow to measure. Instead, it is a result of the method used to compute the anisotropy which will be discussed in detail below. Qualitatively, however, it is clear that the orientational dynamics in the interfacial region are different than in bulk water, and the anisotropy decay suggests that they are slower.

The usefulness of ultrafast infrared spectroscopy is its ability to measure the full time dependence of water orientational motion on the time scale that it actually occurs. In an NMR experiment, the time scale for water reorientation is extracted as a single time constant which is actually related to the time integral of the orientational correlation function.[41] If the decay is not single exponential, the time constant determined from

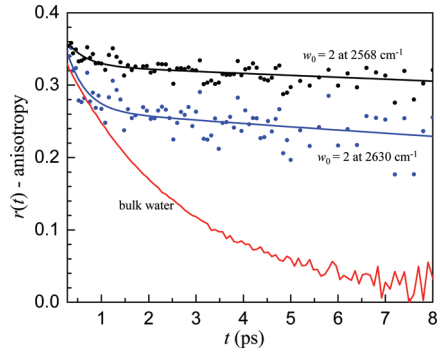

Figure 4. Anisotropy decays at two frequencies in the $w_0 = 2$ reverse micelle with bulk water for comparison. Note the larger amplitude of the fast anisotropy decay at higher frequency in the $w_0 = 2$ reverse micelle.

NMR will be an average over the decay. This is especially critical for interfacial water as demonstrated in Figure 4, which displays the anisotropy decay of water in the $w_0 = 2$ reverse micelle at two frequencies as well as bulk water for comparison. In $w_0 = 2$, there is certainly no core water pool with bulk characteristics; all of the water molecules are either directly interacting with the interface or hydrogen bonded to water molecules that are interacting with the interface. Although there is no bulk water in $w_0 = 2$, there is still a fast component in the anisotropy decay. Moreover, the amplitude of the fast component is wavelength dependent with greater amplitude at higher OD stretching frequencies. Similar fast angular motions of the hydroxyl bond vector were observed in water confined in small reverse micelles by MD simulations.[36]

The fast anisotropy decay is not due to a fraction of the sample completely reorienting on a time scale faster than bulk water. Rather it is caused by local orientational motions of a water molecule within a stable hydrogen-bonding configuration.[11] This type of restricted, incomplete orientational relaxation is referred to as wobbling-in-a-cone.[42] Hydrogen-bond strength is often correlated with the stretching frequency of the OH or OD bond, with weaker hydrogen bonds leading to higher OD stretching frequencies. Weaker hydrogen bonds will result in sampling of a wider range of angles, that is, a larger cone angle. The trend in the amplitude of the fast wobbling motion observed in the $w_0 = 2$ reverse micelle is in line with previous experimental[11] and MD simulation[43] results for bulk water that showed greater inertial orientational motion for molecules with higher OD or OH stretching frequencies. The explanation for this trend is that when hydrogen-bonding interactions are weaker, the angular energy landscape restricting the orientation of the OD or OH to point toward its hydrogen-bond acceptor is flatter, allowing a greater angular deviation. In bulk water, the hydrogen-bond switching rate is fast enough that after the fast inertial reorientation that causes a drop in the anisotropy during the first ~200 fs, no additional fast reorientation is resolvable. However, in the $w_0 = 2$ reverse micelle, the separation of time scales is so great that the wobbling is evident. This wobbling-in-a-cone becomes especially important for describing the dynamics when there is a large separation of time scales between the wobbling and complete hydrogen-bond rearrangement that results in orientational randomization. With this in mind, the orientational dynamics of the interfacial water are likely to have a wavelength-dependent fast wobbling motion as well as a slower, long time reorientation.

On the basis of the blue shift of the IR spectrum and the slowing of the vibrational lifetime and anisotropy decay at higher frequencies it is possible to identify the spectral region most likely to contain interfacial water molecules and examine the nature of their vibrational relaxation and orientational dynamics. In the next section a two-component core/shell model is developed to extract the orientational dynamics of interfacial water molecules. The model is used to fit vibrational population relaxation and anisotropy data in the interfacial spectral region in section C. In section D, the model is tested outside of the interfacial region and possible modifications to the model are discussed.

B. Two-Component Model for Orientational Dynamics. In the Experimental Section, eqs 1 and 2 gave the formulas for the contributions to the pump−probe signal when the probe is resolved parallel and perpendicular to the pump. When there is more than one subensemble in a system and exchange between the ensembles is slow, the contributions of each subensemble to the signal are additive and the population relaxation is simply given by the weighted sum of the population relaxation of the two components.

$$P(t) = aP_1(t) + (1 - a)P_2(t) \tag{5}$$

Here, a is a weighting factor and $P_i(t)$ is the population relaxation of component i. It is important to note that since the pump−probe signal for each component is proportional to $\mu_i^4 c_i$ where μ_i is the transition dipole moment and c_i is the concentration of component i, the weighting factor a depends on both the transition dipole moment and the concentration. If the transition dipole moments of the two subensembles are the same, a is simply related to the fractional concentration of the two species at a particular wavelength. To fit the data, it is not necessary to make any assumptions about the relative transition dipole moments of the ensembles, and in the discussion below, a will simply be treated as a weighting factor.

While the population relaxation behaves in an intuitive manner when more than one subensemble is present, the anisotropy decay becomes quite complicated. To see this we write out the numerator and denominator of eq 4 explicitly.

$$r(t) = \frac{a(I_{\parallel}^1 - I_{\perp}^1) + (1 - a)(I_{\parallel}^2 - I_{\perp}^2)}{a(I_{\parallel}^1 + 2I_{\perp}^1) + (1 - a)(I_{\parallel}^2 + 2I_{\perp}^2)} = 0.4\frac{aP_1(t)C_2^1(t) + (1 - a)P_2(t)C_2^2(t)}{aP_1(t) + (1 - a)P_2(t)} \tag{6}$$

Here, the parallel and perpendicular pump−probe signals due to component i are given by $I_{\parallel}^i$ and $I_{\perp}^i$, respectively, and the orientational correlation functions are given by $C_2^i(t)$. Whereas in the case of a single component the population relaxation divides out of the right-hand side of eq 6, with multiple components the anisotropy decay is not simply a measurement of the orientational correlation function. If the two components have a large separation of time scales for both their vibrational lifetimes and orientational dynamics, then when the fast component has decayed away, the long time anisotropy decay will be an accurate representation of the anisotropy of the slow component. However, at intermediate times the anisotropy decay does not necessarily behave in an intuitive fashion and a model such as eq 6 is required to extract information about the orientational dynamics.

Equations 5 and 6 assume that exchange between the core and the shell is slow compared to the vibrational lifetime and

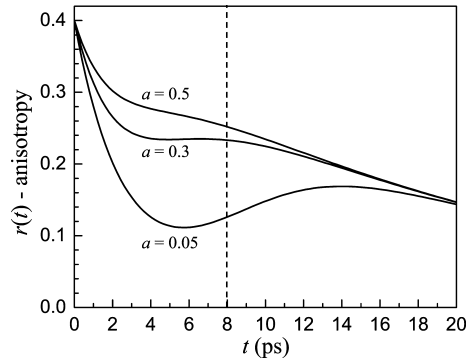

Figure 5. Calculated anisotropy decays of a two-component system with time constants $T_1 = 4.5$ ps, $\tau_r^1 = 20$ ps, $T_2 = 1.8$ ps, and $\tau_r^2 = 2.6$ ps. Three different weighting terms, a, are shown. While the long time anisotropy decays coalesce, the behavior of the curves at intermediate times is not intuitive. The dashed vertical line shows the usual maximum time for experimental data collection. When the anisotropy decays are only analyzed to this point, it appears as though there is a component that does not undergo orientational relaxation.

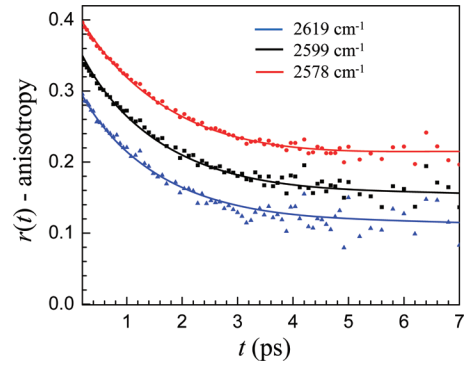

Figure 6. Anisotropy decays and two-component model fits for the $w_0 = 25$ AOT reverse micelle. Three frequencies in the interfacial region are shown. Red circles = 2578 cm^{-1}. Black squares = 2599 cm^{-1}. Blue triangles = 2619 cm^{-1}. The top and bottom data and fits are offset up and down by 0.05, so that the fits can be seen clearly.

orientational time. As discussed in section C below, it is not necessary to include exchange for the experiments analyzed here. Kwak et al. presented a detailed account of the form of the kinetic equations that are necessary when studying chemical exchange with 2D-IR vibrational echo spectroscopy.[44] A recent study of exchange between waters bound to anions and waters hydrogen bonded to other waters determined the exchange rate using 2D-IR spectroscopy and quantitatively analyzed the influence of exchange on vibrational population relaxation and orientational relaxation observables.[45] Therefore, the role that exchange may play in vibrational population relaxation and orientational relaxation measurements is well understood.

Figure 5 shows a series of simulated anisotropy decay curves with all parameters except the weighting term, a, fixed. The parameters were chosen to be representative of bulk water and interfacial water. The vibrational lifetime and orientational relaxation time of component 2 were set to the bulk water values, $T_2 = 1.8$ ps and $\tau_r^2 = 2.6$ ps. The vibrational lifetime and orientational time of component 1 were set at $T_1 = 4.5$ ps and $\tau_r^1 = 20$ ps. In Figure 5 it is clear that at long times the curves coalesce to a single decay, showing that after the fast vibrational lifetime component has decayed the anisotropy decay simply represents the orientational dynamics of the slow component. However, at intermediate times, the anisotropy can behave very strangely, appearing to reach a plateau value for $a = 0.3$ and even turning up for $a = 0.05$.

In spite of the longer vibrational lifetime of the OD stretch of interfacial water molecules, when a significant amount of the water in a reverse micelle is bulk-like, the signal-to-noise ratio of the data begins to deteriorate after ~8 ps, the position of the dashed vertical line in Figure 5. Without the long time decay (>14 ps) to indicate otherwise, the data could be interpreted as reflecting a significant portion (greater than 50% for $a = 0.3$) of nonrotating water molecules even when 70% of the water has bulk characteristics. Previous ultrafast IR experiments of mixtures of water and hydrophobic solutes have observed an offset in the anisotropy decay that was interpreted as an ensemble of rotationally immobilized water molecules.[46,47] This interpretation is in contrast to NMR and MD results that indicate the water around a hydrophobic solute is only slowed by a factor of 1.5−2 from bulk water.[48,49]

As highlighted in Figure 5, when infrared spectroscopy is used to measure the orientational dynamics of two subensembles that have different vibrational lifetimes and orientational dynamics, the anisotropy is not a direct measurement of the orientational dynamics. Recently, ultrafast IR experiments on water−polyether mixtures also found an apparent long time offset for the anisotropy even in dilute mixtures.[50] A two-component model consisting of bulk water and water associated with the polyether described the data extremely well with the fractions of the two components changing in a well-behaved manner with dilution. The orientational relaxation time for water around this large, amphiphilic molecule was ~20 ps.

C. Dynamics of Interfacial Water. In the previous section the importance of the various contributions to the anisotropy decay were highlighted in eq 6. With the many variables, it would be difficult to extract meaningful information from the experimental lifetime and anisotropy decays without fixing some of the parameters. Since the reverse micelles investigated in this report are all quite large, with most of the water well separated from the interface, it is reasonable to believe that this subensemble of water molecules has the properties of bulk water. Therefore, one of the components is assigned the time constants for bulk water, $T_{core} = 1.8$ ps and $\tau_r^{core} = 2.6$ ps. After assigning these two values there are still several unknowns, including the vibrational lifetime and the orientational dynamics of the interfacial water as well as the weighting factor, a. To help determine these values we assume that in the interfacial spectral region the vibrational lifetime and orientational dynamics of the interfacial water are independent of frequency. The population and anisotropy decays at five wavelengths in the interfacial region spanning a range of 40 cm^{-1} are simultaneously fit with the requirement that the vibrational lifetime and orientational relaxation time must be the same for all wavelengths. The weighting factor is allowed to vary with wavelength, reflecting the changing amounts of interfacial vs core water that contribute to the signal at various wavelengths in the interfacial region. Representative fits of several wavelengths in the interfacial region for the $w_0 = 25$ reverse micelle are shown in Figure 6. The vertical scale is correct for the middle curve. The other two curves are offset up and down by 0.05 for clarity. The fits capture the fast initial decay and the plateau. The data for $w_0 = 37$ and 46 reverse micelles have a similar appearance. These larger two reverse micelles have a bigger bulk water contribution to the signal, and the fits show a slight upturning of the anisotropy at long time like that in the middle curve in the simulated data in Figure 5.

The vibrational lifetimes and orientational relaxation times of the interfacial water molecules extracted by fitting the data to the two-component model are given in Table 1. The results

TABLE 1: Vibrational (T_{int}) and Orientational (τ_r^{int}) Relaxation Times for Interfacial Water

	T_{int} (ps)	τ_r^{int} (ps)
$w_0 = 25$	4.3 ± 0.5	19 ± 3
$w_0 = 37$	4.6 ± 0.5	18 ± 3
$w_0 = 46$	3.9 ± 0.5	18 ± 3

TABLE 2: Weighting Factor *a* of the Signal Due to Interfacial Water

	frequency (cm^{-1})				
	2619	2609	2599	2589	2578
$w_0 = 25$	0.35	0.34	0.32	0.29	0.25
$w_0 = 37$	0.20	0.19	0.17	0.16	0.14
$w_0 = 46$	0.19	0.18	0.17	0.15	0.13

demonstrate that in large reverse micelles, the nature of the interface is fairly constant over a range of reverse micelle sizes. The vibrational lifetime of interfacial water is $T_{int} = 4.3 \pm 0.5$ ps, while the orientational time is $\tau_r^{int} = 18 \pm 3$ ps. This orientational relaxation time is consistent with the results of Dokter et al. that gave a lower bound of 15 ps for the orientational relaxation time of HOD in D_2O in AOT reverse micelles.[21]

Table 2 shows how the weighting factor *a* changes with wavelength and radius for the reverse micelles $w_0 = 25$, $r = 4.5$ nm, $w_0 = 37$, $r = 8.5$ nm, and $w_0 = 46$, $r = 10$ nm. As expected, the largest contribution from interfacial water comes at the highest OD stretching frequency for all reverse micelles. The variation in the interfacial weighting factor between reverse micelles is also consistent with a larger proportion of the water interacting with the interface in smaller reverse micelles. In the previous section the possible contribution of orientational wobbling to the anisotropy decay of the interfacial water was discussed. The two largest reverse micelles, $w_0 = 46$ and 37, have such a small amount of interfacial water contributing to the signal that the wobbling motion is not resolvable. However, the $w_0 = 25$ has nearly twice as much interfacial water, and quality fits require including the contribution of wobbling. In the $w_0 = 2$ reverse micelle, the time constant for the fast wobbling motion was between 0.4 and 0.5 ps. Since the wobbling is a local motion that does not depend strongly on the nature of the longer range hydrogen-bonding network, the time scale of this motion should be relatively independent of reverse micelle size, and therefore, the time constant was fixed when determining the wobbling amplitude for the $w_0 = 25$ reverse micelle. For wobbling within an angular cone the amplitude gives a characteristic cone half angle,[42] which ranged from 24° at 2578 cm^{-1} to 28° at 2619 cm^{-1} for $w_0 = 25$. These values lie well within the usual geometric definition of a hydrogen bond and follow the trend expected based on hydrogen-bond strength with a larger angular range allowed for weaker hydrogen bonds (higher OD stretching frequency).

It is important to note that the values for the vibrational lifetimes and orientational relaxation times of interfacial water are almost certainly an average over a distribution of values. The reverse micelle interface is not smooth and featureless but rugged and fluctuating. Water molecules not only interact with sulfonate groups but also sodium counterions and other headgroup moieties such as the ester carbonyls. These different local environments are all likely to have somewhat different vibrational lifetimes and orientational dynamics. Within a small spectral range dominated by the molecules most closely interacting with the surface it is possible to determine representative average values for the vibrational lifetime and orientational relaxation time, but these time constants may not accurately describe the dynamics outside of this region. MD simulations by Faeder and Ladanyi showed that in small reverse micelles the dynamics of water grew progressively and continuously more bulk-like as the distance from the interface increased.[36] It should not be surprising, therefore, if the lifetime and orientational time measured in the interfacial region do not perfectly describe the dynamics of water close to the center of the absorption line. In the next section, data is presented on wavelengths outside of the interfacial region and possible modifications to the two-component model are discussed.

In section B, the possibility of chemical exchange between interfacial and bulk water was mentioned. In a detailed 2D-IR and pump−probe study of ionic solvation shell exchange, Moilanen et al. showed that in concentrated salt solutions, the exchange time for a water molecule to break its hydrogen bond to an anion and form a new hydrogen bond with another water molecule was similar but somewhat slower than the time constant associated with orientational relaxation.[45] A similar conclusion was reached in an MD simulation by Laage and Hynes for water−chloride anion solvation shell exchange at infinite dilution.[51] Water's reorientation mechanism, which involves a large amplitude angular jump from one hydrogen-bond acceptor to another with virtually no time in a non-hydrogen-bonded configuration,[26,27] implies that *reorientation must occur for exchange to occur*. The converse is not true; it is not necessary for exchange to occur every time reorientation occurs. For water at the interface of an AOT reverse micelle, there are multiple binding sites on each sulfonate group and adjacent sulfonate groups are close to one another. Reorientation may take place by forming a new hydrogen bond with a different sulfonate group or at a different binding site on the same sulfonate group without exchanging away from the interface. Water is unique in the strong coupling of its rotational motion to its ability to exchange from one environment to another. It would be unphysical to imagine a water molecule diffusing away from the AOT interface into the bulk-like core without rotating. On the basis of these considerations and the experimental results of chemical exchange in concentrated salt solutions[45] the orientational correlation time of water near solutes and surfaces can be taken as a lower bound for the exchange time. In fact, using MD simulations Faeder and Ladanyi found that the residence times for water molecules at the interface of a $w_0 = 10$ AOT reverse micelles were 18 ps for "bound" water and 34 ps for "trapped" water.[36]

Both the lifetime and orientational relaxation time of water at the AOT interface are slower than those of bulk water. Chemical exchange between interfacial water and the core water, which has bulk properties, would result in apparent vibrational lifetime and orientational relaxation time of the core water being slower than those of bulk water.[45] However, the data for all sizes of reverse micelles and at all wavelengths were fit exceeding well using the bulk water lifetime and orientational relaxation time. Nonetheless, a model that included chemical exchange was used to fit the data presented here but was rejected because the results of the fit were unphysical and necessitated the exchange to occur without water reorientation. For the reasons discussed above, a model including exchange was not used in the data analysis presented here.

D. Dynamics of Water Away from the Interface. At wavelengths outside of the interfacial spectral region, the information content about interfacial water contained in the anisotropy decay rapidly becomes small. It is also quite likely that water with dynamics that are intermediate between those

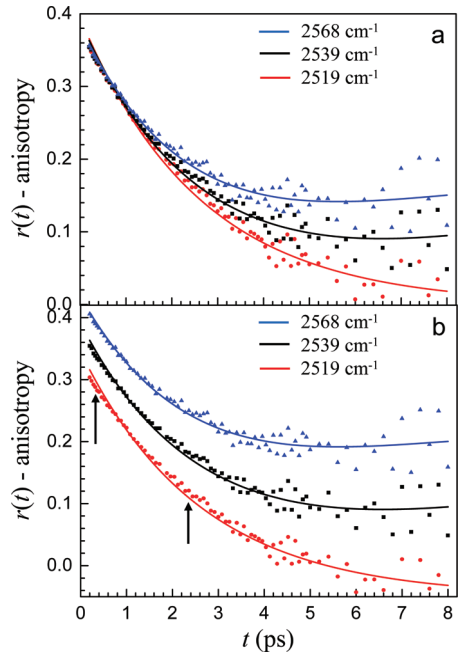

Figure 7. Anisotropy decays and two-component model fits for the $w_0 = 46$ reverse micelle at frequencies outside of the interfacial spectral region. Red circles = 2519 cm^{-1}. Black squares = 2539 cm^{-1}. Blue triangles = 2568 cm^{-1}. (a) Unshifted data and fits to clearly show how the decay slows as the frequency increases. (b) Top and bottom data and fits are offset up and down by 0.05, so that the results can be seen clearly. The fit is quite good at 2568 cm^{-1} but begins to miss at early and intermediate times at lower frequencies as marked by the arrows.

of bulk water and interfacial water contribute to the data. As discussed above, the interfacial water probably has a distribution of orientational relaxation times and vibrational lifetimes representative of the surface heterogeneity. At lower frequencies, toward the center of the line, the tail of the interfacial distribution is probed rather than the center and these molecules may have different dynamics. Figure 7 shows the anisotropy decays for the $w_0 = 46$ reverse micelle at progressively lower frequencies, 2568, 2539, and 2519 cm^{-1}. Figure 7a shows the anisotropy data and the fits using the same time constants as the interfacial region but allowing the weighting factor, a, to vary. Note for the bluer two wavelengths an up turn in the data at long time is evident. This behavior is in accord with the discussion surrounding Figure 5. It is clear from the data in Figure 7a that the anisotropy decays more quickly at the redder wavelengths due to the increasingly bulk-like nature of the water contributing to the signal. Figure 7b shows the same curves with the top and bottom curves offset up and down by 0.05, so that the features of the fit are not masked by the overlapping data. The quality of the fits is reasonably good for all the wavelengths, particularly in light of the fact that there is only one adjustable parameter, the fraction of interfacial water. All of the other parameters are fixed. However, it is clear that the model does not perfectly reproduce the data at 2519 cm^{-1} and to a lesser extent the data at 2539 cm^{-1}. The calculated curves miss at both early and intermediate times as indicated by the arrows in the figure. Although there is certainly a large contribution due to bulk-like water at 2519 cm^{-1}, a comparison of the data with the anisotropy decay of bulk water at the same frequency in Figure 3 makes it clear that the anisotropy decays are not identical.

The most likely explanation for the difference between the single adjustable parameter fits and the data is that some of the water molecules contributing to the signal at the redder wavelengths have dynamics that are intermediate between interfacial water and bulk water. This interpretation is in agreement with earlier MD simulations.[36] While it is apparent that more than one component is contributing to the dynamics in the reverse micelles at lower OD stretching frequencies, the nature of the nonbulk component is no longer solely that of true interfacial water. The logical modification to the two-component model is to allow the vibrational lifetime and orientational time of this nonbulk and noninterfacial component to be faster at wavelengths outside of the interfacial spectral region.

The picture of the interior of large reverse micelles that is coming into focus as a result of MD simulations, and now ultrafast IR spectroscopy is of a core that is very similar to bulk water and an interfacial region that undergoes orientational relaxation that is significantly slower than the core. The interfacial water has a fast wobbling reorientational motion and a long time reorientation approximately seven times slower than bulk water. This long time reorientation is governed by the ability of new hydrogen-bond acceptors to enter the first hydration shell of an interfacial water molecule.[26,49] While MD simulations[49] and NMR experiments[48] of hydrophobic hydration shell dynamics showed a slowing of approximately a factor of 2 in the water dynamics these systems are much different than the reverse micelle interface. The concave curvature and the quasi-two-dimensional extent of a reverse micelle surface are quite different from the hydration shell of a relatively small solute. Not only is the interface effectively fixed on the time scale of the experiment, unlike the relatively fast motions of a small solute molecule, the large extent of the interface also blocks the pathways of new hydrogen-bond acceptors more effectively than a small solute, slowing the time scale of orientational relaxation. In addition, the reverse micelle interface is hydrophilic, leading to a stronger hydrogen-bonding interaction between the water and the interface as compared to the hydrophobic solutes. Laage et. al found that the orientational slowing of water molecules in the solvation shell of solutes was dependent on the strength of the hydrogen bond formed to a hydrophilic moiety.[49] This enthalpic effect may also contribute to the slowing of water reorientation at the interface of AOT reverse micelles.

It is often difficult to obtain an accurate estimate of the extent of the interfacial perturbation. Both MD simulations[2,4] and magnetic relaxation dispersion (MRD) experiments[52] of water hydrating protein surfaces indicate that only the first layer is highly perturbed. MD simulations of water in small reverse micelles also showed that the strongest perturbation was confined to the water molecules directly interacting with the interface.[36] Estimating the extent of the interfacial region from infrared experiments on water in reverse micelles is complicated by the uncertainty in the transition dipole moment alluded to in section B. The infrared absorption at a particular frequency is proportional to $\mu^2 c$, while the pump−probe signal is proportional to $\mu^4 c$. If the transition dipole moments of interfacial water and bulk water are the same at any given frequency, then the frequency-dependent contribution of interfacial water to the signal should be the same for both the infrared spectrum and the pump−probe spectrum.

When dilute HOD is used to probe the dynamics of water at the interface, it is important to note that statistically one-half of the interfacial water molecules will be hydrogen bonding to the interface with their OD and the other half with their OH. This effect is intrinsic to the two-component fitting of the

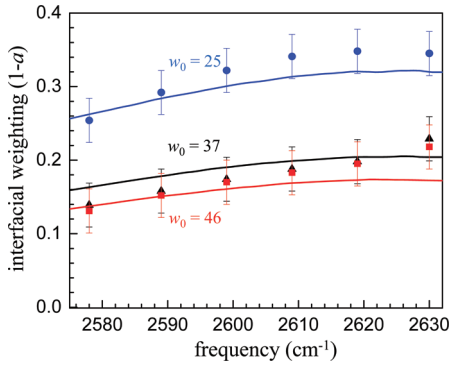

Figure 8. Fraction of the signal due to interfacial water. Solid lines are fractions from fitting the infrared spectrum to a two-component model consisting of bulk water as the core spectrum and $w_0 = 2$ as the interfacial spectrum. The points are the interfacial weight a extracted by simultaneously fitting the vibrational population relaxation and anisotropy decays in the interfacial region to a two-component model. The agreement between the interfacial fractions determined by these two methods indicates that the transition dipole moment of interfacial water and bulk water at a particular frequency is quite similar. Blue line and circles: $w_0 = 25$. Black line and triangles: $w_0 = 37$. Red line and squares: $w_0 = 46$.

infrared spectrum that used the $w_0 = 2$ spectrum to represent the spectrum of interfacial water. In $w_0 = 2$, all of the water molecules are interacting with the interface but not all hydroxyl groups are necessarily hydrogen bonding to a sulfonate. These two different types of hydroxyls are averaged into the spectrum of the interfacial water. A similar averaging effect takes place in extracting the vibrational population relaxation and orientational relaxation of interfacial water. The orientational dynamics of HOD molecules at the interface are perturbed regardless of whether their OH or OD is hydrogen bonded to the sulfonate group because in order for complete reorientation of one of the bond vectors to occur the other must also reorient. Therefore, the long time reorientation of an OD at the interface should be relatively independent of whether it is donating a hydrogen bond to the interface, and small differences are averaged into the time constant extracted for the orientational dynamics of interfacial water. The vibrational population relaxation at the interface may be regarded in a similar manner. The hydrogen-bonding structure at the interface is disrupted by the presence of the interface as well as the sodium counterions. These effects alter the density of states of accepting modes, changing the vibrational population relaxation compared to bulk water. While variation in the vibrational lifetime of an OD is expected based on whether or not it donates a hydrogen bond to the interface, all interfacial ODs are different than bulk ODs and the time constant for vibrational relaxation extracted using the two-component model is necessarily an average over the various configurations. This built in averaging for both the infrared spectrum and the pump−probe data combines the contributions of all ODs in the interfacial shell.

Figure 8 shows the fraction of the signal due to interfacial water from the pump−probe measurements as well as fitting the IR spectra to a superposition of the bulk water spectrum and the $w_0 = 2$ spectrum. The agreement between the two measurements is quite good considering the approximations and assumptions used in the fits. This indicates for the first time that it is reasonable to assume that the transition dipole moments of bulk and interfacial water are not substantially different at any given frequency. Then, based on the integrated areas of the bulk and interfacial fits to the infrared spectrum, it is possible to estimate the fractional concentration of interfacial water.

TABLE 3: Fraction of Interfacial Water from the Infrared Spectrum and a Geometric Model

	IR fraction	geometric fraction
$w_0 = 25$ ($r = 4.5$ nm)	0.17	0.18
$w_0 = 37$ ($r = 8.5$ nm)	0.10	0.10
$w_0 = 46$ ($r = 10$ nm)	0.08	0.08

These values are given in Table 3 for the three reverse micelles as well as the fractional volume contained in a shell of thickness 2.8 Å at the inner surface of a sphere with the same radius as the reverse micelle. A value of 2.8 Å corresponds to the approximate diameter of a water molecule. Even with this very simple model, the agreement between the measured spectra and the geometric model is remarkable, indicating that the most highly perturbed interfacial region appears to be confined to only the first hydration layer at the interface, in agreement with MD simulations and MRD experiments.

IV. Concluding Remarks

We presented a detailed investigation of the interfacial dynamics of water in large AOT reverse micelles. These large reverse micelles have a significant core region of water with dynamics like those of bulk water. The spectral region most likely to contain information about the interfacial dynamics was identified by comparison with the spectrum of the $w_0 = 2$ reverse micelle. It was found that the vibrational lifetime and orientational dynamics slowed in this spectral region, indicating the nature of the interfacial water. A two-component model was developed to extract information about the interfacial water dynamics from the vibrational population relaxation decays and anisotropy decays. While the population relaxation is simply additive when more than one component is present, the anisotropy is more complicated, leading to nonintuitive decay curves (see Figure 5). The dependence of the anisotropy curves on the various input parameters, in particular the weighting factor of the two components, was modeled and discussed.

The two-component model was used to determine the vibrational lifetimes and orientational relaxation times at the interface of large AOT reverse micelles. The results yield a lifetime of 4.3 ps and an orientational relaxation time of 18 ps independent of changes in the radius of the reverse micelle from $r = 4.5$ to 10 nm. Outside of the spectral region that contains significant information about the interface, the two-component model does a reasonable job of describing the dynamics. The discrepancies between the model and the data at lower OD stretching frequencies are most likely caused by the small fraction of interfacial waters contributing to the signal and the possibility that there are water molecules that are not strictly at the interface but are nonetheless influenced by their proximity to the interface. These water molecules may have vibrational lifetimes and orientational relaxation times that are faster than interfacial water. Such water molecules are likely to be found in the low-frequency tail of the spectral distribution of interfacial water and contribute more to the signal as the measurements are made closer to the center of the absorption line.

A comparison of the contribution to the signal from interfacial water molecules in the infrared spectra and the pump−probe spectra indicates that the transition dipole moments of these two species are similar. This allows the fractional concentration of interfacial water to be determined from the integrated area of the interfacial water spectrum (modeled as the $w_0 = 2$ spectrum). On the basis of simple geometric criteria, the data suggest that the most strongly perturbed interfacial water lies in the first hydration layer at the surface.

The results presented here provide a detailed experimental examination of the full time and wavelength dependence of the interfacial water dynamics. We determined the long orientational relaxation time of interfacial waters accurately and show that the orientational wobbling that occurs for water molecules is especially important in the anisotropy decay of interfacial water. These results will provide new benchmarks for future MD simulations of interfacial water.

Acknowledgment. This work was supported by the Department of Energy (DE-FG03-84ER13251), the National Institutes of Health (2-R01-GM061137-09), and the National Science Foundation (DMR 0652232). D.E.M. thanks the National Science Foundation for a Graduate Research Fellowship, and E.E.F. thanks Stanford for a Stanford Graduate Fellowship.

References and Notes

(1) Bhide, S. Y.; Berkowitz, M. L. *J. Chem. Phys.* **2006**, *125*, 094713.
(2) Bagchi, B. *Chem. Rev.* **2005**, *105*, 3197.
(3) Jana, B.; Pal, S.; Bagchi, B. *J. Phys. Chem. B* **2008**, *112*, 9112.
(4) Halle, B.; Davidovic, M. *Proc. Natl. Acad. Sci. U.S.A.* **2003**, *100*, 12135.
(5) Wernet, P.; Nordlund, D.; Bergmann, U.; Cavalleri, M.; Odelius, M.; Ogasawara, H.; Naslund, L. A.; Hirsch, T. K.; Ojamae, L.; Glatzel, P.; Pettersson, L. G. M.; Nilsson, A. *Science* **2004**, *304*, 995.
(6) Shen, Y. R.; Ostroverkhov, V. *Chem. Rev.* **2006**, *106*, 1140.
(7) Modig, K.; Liepinsh, E.; Otting, G.; Halle, B. *J. Am. Chem. Soc.* **2004**, *126*, 102.
(8) Dokter, A. M.; Woutersen, S.; Bakker, H. J. *Phys. Rev. Lett.* **2005**, *94*, 178301.
(9) Rezus, Y. L. A.; Bakker, H. J. *J. Chem. Phys.* **2006**, *125*, 144512.
(10) Cringus, D.; Lindner, J.; Milder, M. T. W.; Pshenichnikov, M. S.; Vohringer, P.; Wiersma, D. A. *Chem. Phys. Lett.* **2005**, *408*, 162.
(11) Moilanen, D. E.; Fenn, E. E.; Lin, Y.-S.; Skinner, J. L.; Bagchi, B.; Fayer, M. D. *Proc. Natl. Acad. Sci.* **2008**, *105*, 5295.
(12) Moilanen, D. E.; Levinger, N. E.; Spry, D. B.; Fayer, M. D. *J. Am. Chem. Soc.* **2007**, *129*, 14311−14318.
(13) Moilanen, D. E.; Piletic, I. R.; Fayer, M. D. *J. Phys. Chem. C* **2007**, *111*, 8884.
(14) Park, S.; Moilanen, D. E.; Fayer, M. D. *J. Phys. Chem. B* **2008**, *112*, 5279.
(15) Piletic, I.; Moilanen, D. E.; Spry, D. B.; Levinger, N. E.; Fayer, M. D. *J. Phys. Chem. A* **2006**, *110*, 4985.
(16) Eaves, J. D.; Loparo, J. J.; Fecko, C. J.; Roberts, S. T.; Tokmakoff, A.; Geissler, P. L. *Proc. Natl. Acad. Sci.* **2005**, *102*, 13019.
(17) Fecko, C. J.; Loparo, J. J.; Roberts, S. T.; Tokmakoff, A. *J. Chem. Phys.* **2005**, *122*, 054506.
(18) Loparo, J. J.; Fecko, C. J.; Eaves, J. D.; Roberts, S. T.; Tokmakoff, A. *Phys. Rev. B* **2004**, *70*, 180201.
(19) Asbury, J. B.; Steinel, T.; Kwak, K.; Corcelli, S. A.; Lawrence, C. P.; Skinner, J. L.; Fayer, M. D. *J. Chem. Phys.* **2004**, *121*, 12431.
(20) Steinel, T.; Asbury, J. B.; Corcelli, S. A.; Lawrence, C. P.; Skinner, J. L.; Fayer, M. D. *Chem. Phys. Lett.* **2004**, *386*, 295.
(21) Dokter, A. M.; Woutersen, S.; Bakker, H. J. *Proc. Natl. Acad. Sci.* **2006**, *103*, 15355.
(22) Cringus, D.; Bakulin, A.; Lindner, J.; Vohringer, P.; Pshenichnikov, M. S.; Wiersma, D. A. *J. Phys. Chem. B* **2007**, *111*, 14193.
(23) Zulauf, M.; Eicke, H.-F. *J. Phys. Chem.* **1979**, *83*, 480.
(24) Venables, D. S.; Huang, K.; Schmuttenmaer, C. A. *J. Phys. Chem. B* **2001**, *105*, 9132.
(25) Rosenfeld, D. E.; Schmuttenmaer, C. A. *J. Phys. Chem. B* **2006**, *110*, 14304.
(26) Laage, D.; Hynes, J. T. *J. Phys. Chem. B* **2008**, *112*, 14230.
(27) Laage, D.; Hynes, J. T. *Science* **2006**, *311*, 832.
(28) Woutersen, S.; Bakker, H. J. *Nature (London)* **1999**, *402*, 507.
(29) Gaffney, K. J.; Piletic, I. R.; Fayer, M. D. *J. Chem. Phys.* **2003**, *118*, 2270.
(30) Tan, H.-S.; Piletic, I. R.; Fayer, M. D. *J. Opt. Soc. Am. B: Opt. Phys.* **2005**, *22*, 2009.
(31) Tokmakoff, A. *J. Chem. Phys.* **1996**, *105*, 1.
(32) Onori, G.; Santucci, A. *J. Phys. Chem.* **1993**, *97*, 5430.
(33) D'Angelo, M.; Onori, G.; Santucci, A. *J. Phys. Chem.* **1994**, *98*, 3189.
(34) Nucci, N. V.; Vanderkooi, J. M. *J. Phys. Chem. B* **2005**, *109*, 18301.
(35) Christopher, D. J.; Yarwood, J.; Belton, P. S.; Hills, B. P. *J. Colloid Interface Sci.* **1992**, *152*, 465.
(36) Faeder, J.; Ladanyi, B. M. *J. Phys. Chem. B* **2000**, *104*, 1033.
(37) Quist, P.-O.; Halle, B. *J. Chem. Soc., Faraday Trans. 1* **1988**, *84*, 1033.
(38) Hauser, H.; Haering, G.; Pande, A.; Luisi, P. L. *J. Phys. Chem.* **1989**, *93*, 7869.
(39) Steinel, T.; Asbury, J. B.; Fayer, M. D. *J. Phys. Chem. A* **2004**, *108*, 10957.
(40) Bakker, H. J.; Woutersen, S.; Nienhuys, H. K. *Chem. Phys.* **2000**, *258*, 233.
(41) Abragam, A. *The Principles of Nuclear Magnetism*; Oxford University Press: Oxford, 1983.
(42) Lipari, G.; Szabo, A. *J. Am. Chem. Soc.* **1982**, *104*, 4546.
(43) Laage, D.; Hynes, J. T. *Chem. Phys. Lett.* **2006**, *433*, 80.
(44) Kwak, K.; Zheng, J.; Cang, H.; Fayer, M. D. *J. Phys. Chem. B* **2006**, *110*, 19998.
(45) Moilanen, D. E.; Wong, D.; Rosenfeld, D. E.; Fenn, E. E.; Fayer, M. D. *Proc. Natl. Acad. Sci. U.S.A.* **2009**, *106*, 375.
(46) Rezus, Y. L. A.; Bakker, H. J. *Phys. Rev. Lett.* **2007**, *99*, 148301.
(47) Rezus, Y. L. A.; Bakker, H. J. *J. Phys. Chem. A* **2008**, *112*, 2355.
(48) Qvist, J.; Halle, B. *J. Am. Chem. Soc.* **2008**, *130*, 10345.
(49) Laage, D.; Stirnemann, G.; Hynes, J. T. *J. Phys. Chem. B* **2009**, *113*, 2428.
(50) Fenn, E. E.; Moilanen, D. E.; Levinger, N. E.; Fayer, M. D. *J. Am. Chem. Soc.* **2009**, *131*, 5530−5539.
(51) Laage, D.; Hynes, J. T. *Proc. Natl. Acad. Sci.* **2007**, *104*, 11167.
(52) Halle, B. *Philos. Trans. R. Soc. London B* **2004**, *359*, 1207.

JP902004R